

Amorphous ferromagnetic Ag-X ($X = \text{Ni, Co, Gd}$) alloys

J. J. Hauser

Bell Laboratories, Murray Hill, New Jersey 07974

(Received 2 June 1975)

The Curie points (T_C) of amorphous Ag-X ($X = \text{Ni, Co, Gd}$) films prepared by getter sputtering on substrates held at 77°K, were determined without warming up the films above 77°K. As revealed by susceptibility and electrical measurements, the films remain unchanged up to 220°K; above this temperature one observes an irreversible decrease in resistivity accompanied by an irreversible increase in T_C although the films are still amorphous at room temperature. The critical concentration for the appearance of ferromagnetism (41-at.% Ni) and the increase of T_C with Ni concentration ($\approx 9^\circ\text{K/at.}\%$) are quite close to the values reported for crystalline Ni-Cu alloys. These results suggest again the validity of the virtual-bound-state model over the rigid-band model and confirm that clustering is not a major factor in crystalline Cu-Ni alloys. An extrapolation of the present experiments to pure Ni leads to a T_C of about 540°K for amorphous Ni. The validity of this extrapolation is supported by Ag-Co and Ag-Gd experiments.

I. INTRODUCTION

The validity of the virtual-bound-state model over the rigid-band model in Cu-Ni alloys was suggested theoretically by Land and Ehrenreich¹ and experimentally by the optical data of Seib and Spicer.² The validity of this conclusion was questioned on the basis that clustering could exist in such alloys.³ Although this criticism was rejected with the help of neutron scattering experiments,^{4,5} the possibility of clustering in alloys obtained by conventional metallurgy has been raised numerous times.⁶⁻⁸ More recently, x-ray photoelectron spectroscopy experiments⁸ have established again the validity of the virtual-bound-state model for Cu-Ni alloys but these experiments could still have been influenced by the presence of clustering. One way to obviate this difficulty is to prepare amorphous alloys by low-temperature film deposition, where one can expect a random distribution of atoms. This technique is also attractive from the point of view that many metastable alloys, not attainable by conventional metallurgy, can be prepared in this manner. In order to select elements likely to result in amorphous films, one can follow the rule suggested by Mader⁹: the atomic radii of the components should differ by at least 10%. An alternate rule based on the same physical principles is to choose elements with a liquid miscibility gap in their phase-equilibrium diagram. With these ideas in mind, we chose Ag-Ni, Ag-Co, and Ag-Fe alloys, where the radius of the magnetic atom is approximately 15% smaller than that of Ag, and the Ag-Gd alloy system, where the atomic radius of Gd is 25% larger than that of Ag. This study will be divided into three parts: The first part will deal with the sample analyses; in the second part the degree of amorphousness and

the compositional range of the amorphous state will be discussed for the various alloys; in the third part the compositional dependence of the Curie temperatures will be examined in terms of previous experiments and existing models.

II. EXPERIMENTAL PROCEDURE

All amorphous alloy films of the present study were getter sputtered at 2 W (1000 V, 2mA) onto sapphire substrates held at 77°K from a cold-pressed powder target. The deposition time was usually 6 h, which at the average deposition rate of 30 Å/min resulted in an average film thickness of about 1 μm. In order to ensure the best statistical mixing of the two component powders, it is best to use the finest powder available (e.g., 325 mesh). In the case of Ag and Ni, 325- and 200-mesh powders were used for both; for Ag-Co, Ag-Fe, and Ag-Gd experiments, the Ag powder was always 325 mesh, as were the Co and Fe powders, but the Gd powder was only 40 mesh. The powders were then mixed and tumbled and finally cold pressed in the form of a disk. An estimate of the composition to be expected from this target can be obtained from x-ray fluorescence counts for both components taken directly on the as-pressed disk. The composition of the films was ascertained by x-ray fluorescence analysis and by Coprex analysis.¹⁰ The amorphous nature of the films was established with the help of an x-ray diffraction trace which could be obtained without warming up the sample above 77°K. The Curie points (T_C) of the films were determined by susceptibility measurements using a sensitive ac bridge with two balanced coils. The bridge was operated at 10 000 Hz with 2.5 V, which corresponds to a modulating field of 4 Oe. The sample

was mounted in the susceptibility holder under liquid nitrogen without being warmed up above 77 °K; the T_C could be measured with or without an externally applied magnetic field.

III. EXPERIMENTAL RESULTS AND DISCUSSION

A. Sample analyses

The composition of the targets obtained by x-ray fluorescence analysis is listed in Table I for both 325-mesh powders [Table I(a)] and 200-mesh powders [Table I(b)]. The x-ray fluorescence analysis was calibrated by obtaining the actual composition of a film (deposited with the 50-at. % nominal target) by Coprex analysis. The composition of all other films was then determined as 90% of the fractional Ni counts.¹¹ As sputtering is a steady-state process one expects the composition of the

films to be close to that of the sputtering target. The accuracy in determining the concentration of the film will depend of course on how precisely the composition of the target is known, which in turn is best established¹² for powders with the smallest particle size (e.g., 325 mesh). This fact is well established in Table I, where one can observe that for the 325-mesh powders the experimental concentration is very close to the nominal concentration ($\pm 10\%$) over the whole concentration range. On the other hand, the experimental concentration is systematically larger than the nominal concentration for the 200-mesh powders [Table I(b)] and sometimes by as much as 60%. Consequently, the film composition is much less reliable in the 200-mesh experiments than in the 325-mesh experiments. Furthermore, it is clear from Table I that compositional variations of the

TABLE I. X-ray fluorescence analysis of Ag-Ni sputtering targets.

Nominal Ni concentration (at. %)	Ag counts	Ni counts	Experimental concentration ^a (at. %)
	(a) 325-mesh powders		
30	9035	4112	28
40	8061	5908	38
40	7820	6400	41
45	8135	6672	41
45 ^b	7591	7965	46
45	7360	7400	45
45 ^b	7065	9002	50
50	7305	7866	47 ^a
50 ^b	7007	8353	49
55	7014	9824	53
55 ^b	6236	10866	57
75	4071	16403	72
	(b) 200-mesh powders		
20	23709	12803	32
25	21937	16494	39
28	21795	17485	40
28 ^b	21337	20206	44
33	21121	21641	46
33 ^c	20965	20062	44
35	20379	20267	45
35 ^c	19816	16254	41
35	19591	23468	49
35 ^b	19269	29378	54
40	19533	24520	50
40	18717	30464	56
44	17878	36709	61
45	18130	27418	54
50	17620	31293	58
50	17467	29702	57
50 ^b	18767	22422	49

^a Experimental concentration is calibrated by directly obtaining the composition of one film by Coprex analysis, which leads to the result that the experimental concentration is equal to 0.9 times the fractional Ni counts (Ref. 11).

^b Second side of the same disk of sputtering target.

^c Same side of disk after removing about 1 mm by polishing.

order of 10% can occur from one side of the target to the other or even at a small depth below the as-pressed surface. Taking all these facts into account, the composition of the films cannot be ascertained to better than $\pm 5\%$ even in the most favorable case (325-mesh powders). As we shall see later, this compositional uncertainty is sufficient to explain both the scatter in the data and the temperature width of the ferromagnetic transitions.

The x-ray fluorescence analyses for Ag-Fe and Ag-Co 325-mesh powder targets gave essentially similar results to those shown above for Ag-Ni and will therefore not be discussed in further detail. On the other hand, in the case of Ag-Gd experiments, the finest-particle Gd powder available was only 40 mesh and consequently an x-ray fluorescence analysis on the as-pressed targets could be quite unreliable in view of the above discussion on 200-mesh Ag-Ni powders. As a result, the composition of each Ag-Gd film was directly determined by Coprex analysis.

B. Amorphous structure of films

The following structural study on Ag alloy films will establish again the validity of Mader's suggestions for the formation of an amorphous solution: The atomic radii of the two components must differ by more than 10% and the films must be deposited at a sufficiently low temperature. Even under these favorable conditions, the amorphous solid solutions exist only in a restricted compositional range.⁹ In the case of Ag-Ni alloys, where the Ag atom is about 15% larger than the Ni atom, one obtains at 77 °K, as shown in Fig. 1, an amorphous film. This film remains amorphous upon warming up to room temperature except for an increase in density of about 20% (as shown by the displacement of the lines towards larger angle). These sputtered films are quite stable against recrystallization undoubtedly because of the pinning effect of argon atoms; one has to anneal for 1 h at 500 °C to get appreciable recrystallization in the form of small Ag and Ni crystallites with a (111) preferred orientation (see insert of Fig. 1). These amorphous solid solutions can be obtained with Ni ranging from 32 to 61 at.%, which is in good agreement with results on similar Cu-Ag amorphous solutions.^{9,13} On the other hand, Cu-Ni films deposited under identical conditions were microcrystalline with a 55-Å particle size. This is in agreement with similar Cu-Co films,^{9,13,14} where just as for Cu-Ni the two component atoms have approximately the same radius, thus showing that a low temperature of deposition is not sufficient by itself.

In the case of Co-Ag, where the difference in

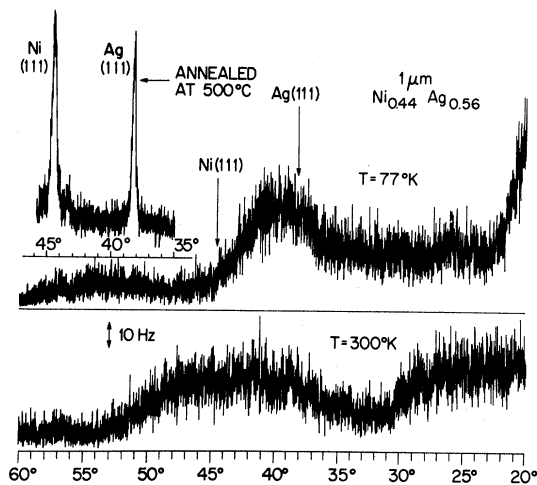


FIG. 1. X-ray diffractometer traces for a $\text{Ni}_{0.44}\text{Ag}_{0.56}$ film; upper trace taken on as-deposited film at 77 °K, bottom trace obtained at 300 °K; upper-left insert shows recrystallization as a result of 500 °C anneal. Crystalline lines are indicated by arrows.

atomic radii is also 15%, one expects again amorphous films. This is demonstrated for a $\text{Co}_{0.41}\text{Ag}_{0.59}$ film in Fig. 2. As the Co content is reduced, one loses the amorphous structure and microcrystallinity appears as shown by Fig. 3 and 4. The pattern of Fig. 3 for the 28-at.% Co solution is still representative of a mostly amorphous film with small (≈ 50 Å) Ag crystallites with a (111) preferred orientation. The films become even more crystalline, as evidenced by the larger Ag crystallites (≈ 100 Å) shown in Fig. 4, for the 18-at.% Co solution. Consequently, in the range of compositions pertinent to the magnetic studies (15–21-at.% Co) the films are not amorphous but microcrystalline. However, as shown in the case of similar Cu-Co films,¹⁴ such microcrystalline films can still be considered as random solid solutions.

Amorphous Ag-Gd films were obtained in a wide range of Gd concentrations (20–70 at.%). This result is not surprising in view of the fact that the

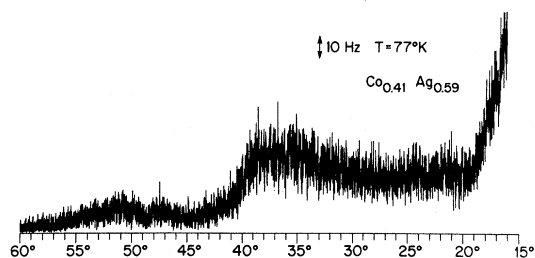


FIG. 2. X-ray diffractometer trace taken on as-deposited $\text{Co}_{0.41}\text{Ag}_{0.59}$ film at 77 °K.

atomic radius of Gd is 25% larger than that of Ag. Furthermore, the x-ray diffractometer trace for pure-Gd films deposited at 77 °K is very similar to that shown for $\text{Co}_{0.28}\text{Ag}_{0.72}$ films in Fig. 3 and can be interpreted as a mixture of amorphous phase and 60-Å Gd microcrystals.

C. Compositional dependence of Curie temperatures

The dependence of the Curie temperature (T_C) of amorphous Ag-Ni alloy films on Ni concentration is shown in Fig. 5. Although the data for the 200- and 325-mesh powders are quite close, we shall ignore the 200-mesh data, which as discussed above are less reliable. The ferromagnetic transitions are relatively wide for all films, the transition width increasing from about 10 °K to several tens as the Ni content increases from 40 to 60 at.%. Considering the steep slope of Fig. 5 (9 °K/at. %), this transition width corresponds to spreads in concentration of the order of 1-5 at.%. Such variations in concentration can be expected on the surface of the target and across its thickness (see Table I). At any rate, the Curie temperature was defined as the temperature at which no ferromagnetism remains. Other definitions such as the middle of the transition or the onset of the transition leave the data shown in Fig. 5 essentially unchanged. The straight line drawn through the data of Fig. 5 was obtained by a least-squares fit, which results in $T_C = 0$ °K (onset of ferromagnetism) at 41-at.% Ni and a concentration dependence of the Curie temperature of 9.1 °K/at.%. The scatter about the solid line is consistent with the previously discussed compositional uncertainties. The data shown in Fig. 5 terminate at 61-at.% Ni ($T_C \approx 200$ °K) for the following two reasons. First, between 61- and 75-at.% Ni the films change from amorphous to microcrystalline. Second, although as discussed in

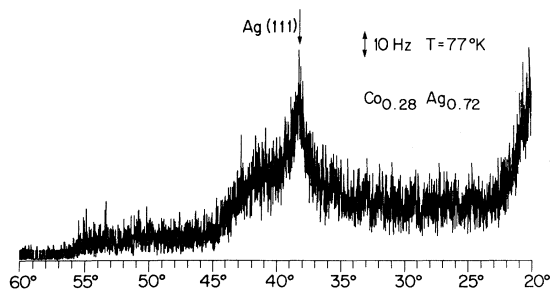


FIG. 3. X-ray diffractometer trace taken on as-deposited $\text{Co}_{0.28}\text{Ag}_{0.72}$ film at 77 °K showing the presence of small Ag microcrystals (≈ 50 Å) in an amorphous matrix.

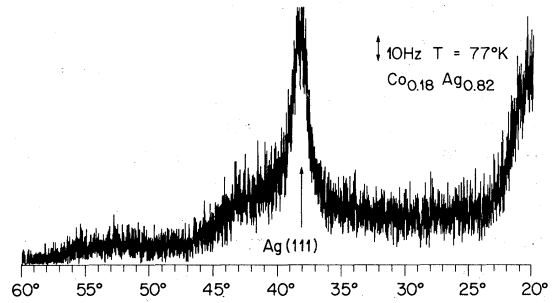


FIG. 4. X-ray diffractometer trace taken on as-deposited $\text{Co}_{0.18}\text{Ag}_{0.82}$ film at 77 °K showing the presence of small Ag microcrystals (≈ 100 Å) in an amorphous matrix.

the structure section of this paper the films remain amorphous at room temperature (Fig. 1), there are irreversible changes occurring at about 210 °K. To be specific, the resistivity of a $\text{Ag}_{0.5}\text{Ni}_{0.5}$ film which was $1.7 \times 10^{-3} \Omega \text{ cm}$ at 77 °K started to decrease at 210 °K to reach a value of $1.3 \times 10^{-3} \Omega \text{ cm}$ at room temperature. After overnight anneal at room temperature, the resistivity further decreased to $1.1 \times 10^{-3} \Omega \text{ cm}$, which corresponds to a mean free path of about 1 Å. The irreversible decrease of the resistivity at 210 °K is

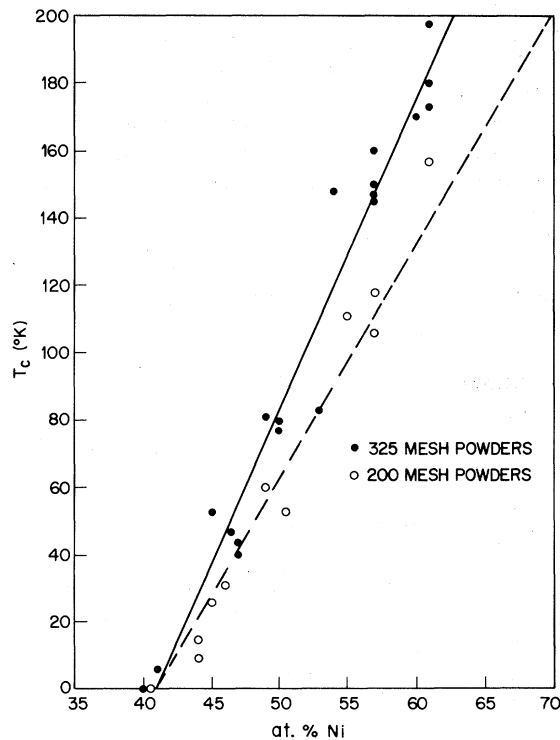


FIG. 5. Compositional dependence of the Curie temperature (T_C) for amorphous Ag-Ni alloy films.

accompanied by an irreversible increase of the Curie temperature. This increase in Curie temperature is consistent with the increase in density observed in the x-ray diffractions (Fig. 1). Anyhow, the data shown in Fig. 5 are entirely reliable as they are free of such annealing effects. The data shown in Fig. 5 are very similar to that obtained on well-annealed crystalline Cu-Ni alloys; namely, the onset of ferromagnetism at 41-at. % Ni is close to the threshold of 44-at. % Ni in Cu-Ni alloys¹⁵ and the slope of Fig. 5 ($9^\circ\text{K/at.}\%$) is in good agreement with a slope of about $8^\circ\text{K/at.}\%$ for Cu-Ni alloys.¹⁵ One may conclude from this close similarity between amorphous and crystalline alloys that, in agreement with Moss,⁵ clustering effects must be quite small in well-annealed Cu-Ni alloys. Consequently, the validity of the virtual-bound-state model over the rigid-band model should not be in doubt³ on the basis of possible clustering. Furthermore, when nickel, which has one less electron than copper or silver in the outermost shells, is alloyed with Cu or Ag, the rigid-band model predicts that the *s-p* bands should empty progressively, thus decreasing the *d*-band-to-Fermi-level energy separation. At some nickel concentration, the Fermi level should coincide with the top of the *d* band, at which point the alloy becomes ferromagnetic. As the top of the *d* band in Ag is about 4 eV below the Fermi level as compared to 2 eV in the case of Cu,⁸ one would expect if the rigid-band model were to apply that ferromagnetism would appear at a lower Ni concentration in Cu-Ni alloys than in Ag-Ni alloys, which is directly contradicted by the present experiments ($T_C = 0^\circ\text{K}$ at 41 at. % for Ag-Ni and 44 at. % for Cu-Ni).

Besides the validity of the virtual-bound-state model, one can draw other interesting conclusions from these amorphous alloys. In particular, an extrapolation of the solid line of Fig. 5 to pure Ni leads to a T_C of about 540°K for amorphous Ni. The difference in density between as-deposited and annealed Ag-Ni films is sufficient alone to explain the lower T_C of amorphous Ni as compared to that of crystalline Ni (631°K). Using the relation

$$\Delta T_C = \frac{dT_C}{dP} \cdot V \frac{dP}{dV} \frac{\Delta V}{V} \quad (1)$$

with a bulk modulus¹⁶ of 1.7×10^{12} dyn/cm² and the experimental value¹⁷ for dT_C/dP of 3.5×10^{-4} K/atm, the 20% increase in density which occurs upon annealing to room temperature corresponds to a 120°K increase in T_C . This extrapolated value of 540°K for the T_C of amorphous Ni should be treated cautiously in view of other studies on amorphous ferromagnets. The first example of an amorphous ferromagnet was a Co-Au alloy¹⁸

soon followed by quenched evaporated¹⁹ PdSi-*X* alloys (*X* = Fe, Co, Ni). However, while the Fe and Co alloys were ferromagnetic at room temperature, nothing was stated about the Ni alloy. Furthermore, amorphous Ni films obtained by evaporation on liquid-helium-cooled substrates²⁰ were not ferromagnetic at room temperature and the situation is unclear in amorphous Ni films sputtered in hydrogen at room temperature.^{21,22} Amorphous Ni_{0.90}Co_{0.10} films obtained by sputtering at 95°K have a room-temperature resistivity of $780 \mu\Omega\text{ cm}$, which is very close to that of the hydrogen-sputtered films²² ($740 \mu\Omega\text{ cm}$) and are not ferromagnetic. It would therefore appear that ferromagnetism in amorphous materials depends on the method of attaining the amorphous state. Nevertheless, the validity of the present extrapolation can be justified by similar experiments on other amorphous alloys. The compositional dependence of the Curie temperature for microcrystalline Ag-Co alloy films (and one Ag-Fe film) is shown in Fig. 6. The onset of ferromagnetism at low Co concentration (15 at. %) reflects the high Co moment, while the steep concentration dependence ($40^\circ\text{K/at.}\%$) is the result of the high T_C 's of Co (1400°K) and Fe (1043°K). The comparison with Ag-Ni amorphous alloys is felt to be valid

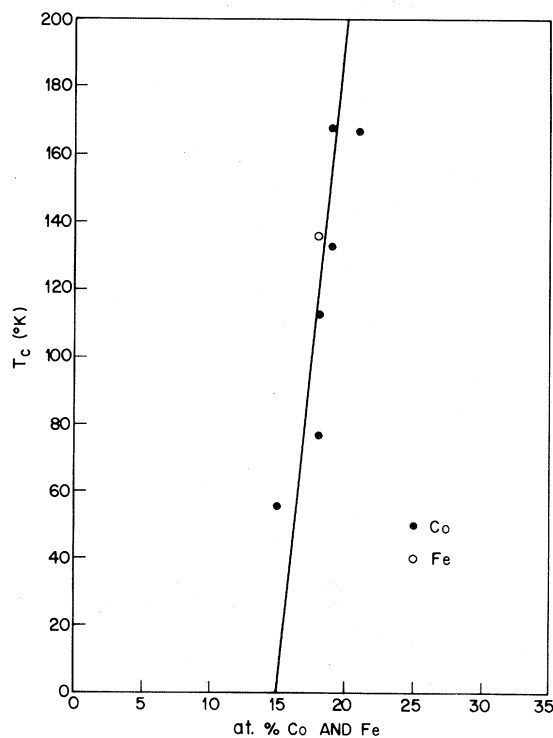


FIG. 6. Compositional dependence of the Curie temperature (T_C) for quasiamorphous (microcrystalline) Ag-Co and Ag-Fe alloy films.

despite the fact that the Ag-Co films are microcrystalline (Fig. 4) because such films can still be considered as random solid solutions.¹⁴ The compositional dependence of the Curie temperature for amorphous Ag-Gd alloy films is shown in Fig. 7. This system is particularly informative as amorphous ferromagnetism can be studied over the complete compositional range. The only exception is the pure-Gd film, which is only quasi-amorphous, i.e., a mixture of 60-Å microcrystals embedded in an amorphous matrix. As a result, the ferromagnetic transition of the Gd film is relatively wide, spreading from 290 (the T_C of crystalline Gd) to 253 °K. Consequently, the value of 253 °K was chosen as the T_C for amorphous Gd. It is clear from Fig. 7 that the line which best averages the data for amorphous Ag-Gd films (with a slope of 3 °K/at.%) passes through the datum point for pure Gd. One may therefore conclude from the study of these three Ag alloy systems that the extrapolated T_C of 540 °K for amorphous nickel is a reasonable extrapolation.

ACKNOWLEDGMENTS

I would like to thank C. M. Antosh for his able technical assistance and J. E. Kessler for his help with the Coprex analysis.

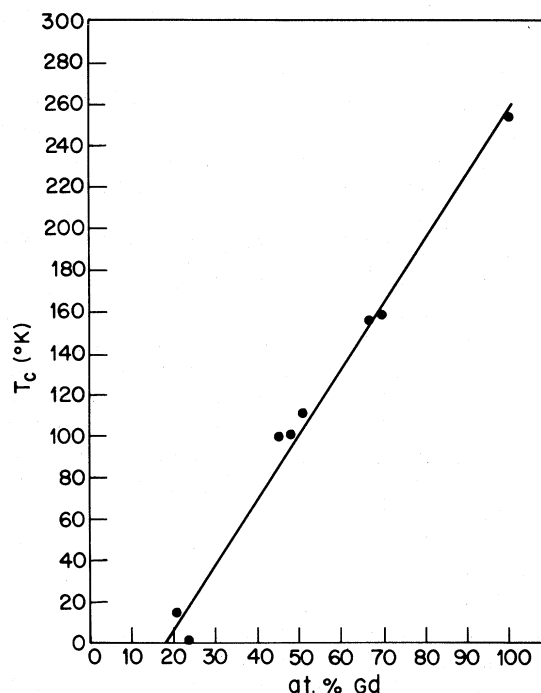


FIG. 7. Compositional dependence of the Curie temperature (T_C) for amorphous Ag-Gd alloy films.

¹N. D. Lang and H. Ehrenreich, *Phys. Rev.* **168**, 605 (1968).

²D. H. Seib and W. E. Spicer, *Phys. Rev. Lett.* **20**, 1441 (1968).

³A. Kidron, *Phys. Rev. Lett.* **22**, 774 (1969).

⁴B. Mozer, D. T. Keating, and S. C. Moss, *Phys. Rev.* **175**, 868 (1968).

⁵S. C. Moss, *Phys. Rev. Lett.* **23**, 381 (1969).

⁶L. H. Bennett, L. J. Swartzendruber, and R. E. Watson, *Phys. Rev. Lett.* **23**, 1171 (1969).

⁷B. Window and C. E. Johnson, *Phys. Rev. Lett. A* **29**, 703 (1969).

⁸S. Hüfner, G. K. Wertheim, and J. H. Wernick, *Phys. Rev. B* **8**, 4511 (1973).

⁹S. Mader, *J. Vac. Sci. Techn.* **2**, 35 (1965).

¹⁰I am indebted to J. E. Kessler for his help in performing the Coprex analysis.

¹¹The fractional Ni counts are equal to: (Ni counts)/(Ni

counts plus Ag counts).

¹²J. J. Hauser, *Phys. Rev. B* **5**, 1830 (1972).

¹³S. Mader, H. Widmer, F. M. d'Heurle, and A. S. Nowick, *Appl. Phys. Lett.* **3**, 201 (1963).

¹⁴E. Kneller, *J. Appl. Phys.* **33**, 1355 (1962).

¹⁵T. J. Hicks, B. Rainford, J. S. Kouvel, G. G. Low, and J. B. Comly, *Phys. Rev. Lett.* **22**, 531 (1969).

¹⁶W. H. J. Childs, *Physical Constants* (Methuen, London, 1958), p. 20.

¹⁷L. Patrick, *Phys. Rev.* **93**, 384 (1954).

¹⁸S. Mader and A. S. Nowick, *Appl. Phys. Lett.* **7**, 57 (1965).

¹⁹C. C. Tsuei and L. Duwez, *J. Appl. Phys.* **37**, 435 (1966).

²⁰J. R. Bosnell, *Thin Solid Films* **3**, 233 (1969).

²¹A. Colombani, *C. R. Acad. Sci. (Paris)* **208**, 795 (1939).

²²A. Colombani, *Ann. Phys. (Paris)* **19**, 272 (1944).